Marine Chemistry 213 (2019) 40–48

Contents lists available at ScienceDirect

Marine Chemistry

journal homepage: www.elsevier.com/locate/marchem

Production of tyrosine-like fluorescence and labile chromophoric dissolved organic matter (DOM) and low surface accumulation of low molecular weight-dominated DOM in a productive Antarctic sea

Meilian Chen[a,b], Jinyoung Jung[c], Yun Kyung Lee[a], Tae-Wan Kim[c], Jin Hur[a,*]

[a] Department of Environment & Energy, Sejong University, Seoul 05006, South Korea
[b] Environmental Program, Guangdong Technion - Israel Institute of Technology, Shantou 515063, China
[c] Division of Polar Ocean Environment, Korea Polar Research Institute, Incheon 21990, South Korea

ARTICLE INFO

Keywords:
Dissolved organic matter (DOM)
Chromophoric DOM production
Net DOC production ratio,EEM-PARAFAC
SEC-OCD
Amundsen sea

ABSTRACT

The Antarctic seas play critical roles in global carbon cycling. Yet, little is known about the dissolved organic matter (DOM) characteristics and the dynamics there. Here, we conducted an extensive study on the seawater DOM in the Amundsen Sea in the Pacific sector of the Southern Ocean. We found that low molecular weight fractions quantitatively dominated the DOM composition at the surface of the highly productive Amundsen Sea Polynya with the relative abundance reaching up to ~89%. Moreover, CDOM and tyrosine-like fluorescence generation were observed, with the average values of~2.4–2.6 m^{-1} (a_{254}) and ~0.3 RU, respectively. While there is a net positive accumulation of dissolved organic carbon (DOC) at the ocean's surface, the net accumulation was negative for the chromophoric DOM (CDOM), which suggests a labile nature for the freshly produced CDOM. The estimated net DOC production ratio was only ~9 ± 6%, which was less than the global level (~17%). This finding signified a low surface accumulation of DOM in the austral summer, which is potentially explained by its nonlimiting nutrients, photo- and/or bio-labile nature of produced DOM, and long water residence time.

1. Introduction

The Antarctic region, which is vulnerable to the ongoing climate change, plays pivotal roles in global hydrological and biogeochemical cycles. > 70% of world's freshwater is stored in the glaciers in the Antarctic areas (Fretwell et al., 2013). The Antarctic ice sheet alone contains ~3.3–8.4 Gt of organic carbon (Smith et al., 2017). The global oceans sink is ~48% of the total anthropogenic CO_2 emissions (Sabine et al., 2004), while the Southern Ocean' role is disproportionately important relative to its size, which accounts for > 40% of the global oceanic anthropogenic CO_2 uptake (Sallee et al., 2012). It also serves as a major site of world ocean deep water upwelling (~80%) via spiraling pathways (Tamsitt et al., 2017). In particular, the coastal Southern Ocean has been reported as a strong carbon sink (Arrigo et al., 2008). Nevertheless, the dissolved organic matter (DOM) characteristics and the dynamics in this region are still poorly understood.

The Amundsen Sea in the west Antarctica has undergone a rapid ice loss through basal melting due to the warm Circumpolar Deep Water (CDW) intrusion channeled through the bathymetric cross-shelf troughs. It alone contributes ~10% to the global sea level rise (Mouginot et al., 2014; Turner et al., 2017). The Amundsen Sea Polynya (ASP) was reported as the greenest and the most productive region among the coastal polynyas around Antarctica that are fueled by iron from the melting glaciers (Arrigo and van Dijken, 2003). Recently, a low particulate organic carbon (POC) export to the seafloor (< 5% of primary productivity) was reported in the highly productive (> 200 mmol C m^{-2} d^{-1}, Yager et al., 2016) coastal Amundsen Sea in the Southern Ocean, which was explained by the off-shelf flushing of the carbon-enriched waters due to the lack of deep water formation caused by the intrusion of warm CDW (Lee et al., 2017). The Southern Ocean has no major terrestrial inputs of DOM. Hence, in situ primary productivity is the main source of organic matter in the surface ocean although the dissolved organic carbon (DOC) concentrations in the deep waters are primarily controlled by allochthonous processes (Bercovici and Hansell, 2016). In addition, microbes have been reported to play a critical role in glacial environments, which include supra-, en-, and sub-glacial, by the microbial formation of labile organic carbon (Smith et al., 2017; Musilova et al., 2017).

* Corresponding author.
E-mail address: jinhur@sejong.ac.kr (J. Hur).

https://doi.org/10.1016/j.marchem.2019.04.009
Received 5 September 2018; Received in revised form 20 April 2019; Accepted 22 April 2019
Available online 24 April 2019
0304-4203/

In the recent DOM studies in the Southern Ocean, notable findings are chromophoric DOM (CDOM) production and a high protein allocation (~60% protein out of the total photosynthetic organic carbon) of phytoplankton in the Amundsen Sea Polynya (Lee et al., 2016; Song et al., 2016). High levels of CDOM and the biogeneration of CDOM were also observed in the Amundsen and Bellingshausen Seas in the Southern Ocean (Ortega-Retuerta et al., 2009; Lee et al., 2016; Song et al., 2016). High bioavailability of DOM produced in phytoplankton bloom has also been suggested (Kähler et al., 1997; Carlson et al., 1998).

Semilabile DOC, which survives a rapid turnover and accumulates in the surface of the ocean over the timescale of months to years, is an important element for the marine carbon cycle via vertical (wintertime convective overturn) and horizontal exports (advection) (Hansell and Carlson, 1998). The contribution of semilabile DOC in the surface ocean was estimated to be ~17% of the global net community production (Hansell and Carlson, 1998; Romera-Castillo et al., 2016). In the Antarctic seas, the Ross Sea showed quite some variability in surface semilabile DOC accumulation during spring bloom (~4–20%, Carlson et al., 1998; Hansell and Carlson, 1998). Furthermore, the newly produced DOC was found to be bio-labile in the Ross Sea with > 70% of it utilized by bacteria over the course of 19 days, indicative of low surface DOC accumulation despite the high primary productivity (Carlson et al., 1998).

This study mainly aimed to investigate the dynamics of DOM in the Antarctic region by utilizing multiple DOM fingerprints. The specific objective was to estimate the DOM accumulation in the marine surface and the potential export to the deep ocean. We utilized excitation emission matrix coupled with parallel factor analysis (EEM-PARAFAC), a high-resolution Fourier transform ion cyclotron resonance mass spectrometry (FT-ICR-MS), and a size exclusion chromatography coupled with an organic carbon detector (SEC-OCD), in order to gain in-depth information on DOM characteristics and dynamics. Furthermore, we calculated the net DOC production ratio (NDPr) using the net DOC accumulation on the surface waters divided by the net community production estimated from the nutrients drawdown. The highly productive Amundsen Sea fueled by iron from melting glaciers was chosen for this study (Alderkamp et al., 2015). Sampling in the Amundsen Sea is sparse for DOM studies due to remoteness and harsh environments. This is the first report of fluorescent, size distribution, and molecular fingerprints there. The marine-ice-sheet instability is underway throughout the Amundsen Sea embayment due to the warm Circumpolar Deep Water (CDW) intrusion (St-Laurent et al., 2013), which alone could contribute to more than one meter of sea-level rise if melted (Ritz et al., 2015).

2. Methods

2.1. Site description and water mass properties

Sampling sites are located in the Amundsen Sea of Antarctica (Fig. 1). The sea ice concentration data from January 14th to February 3rd, 2016, in the Antarctic can be obtained from the website http://www.meereisportal.de. The warm CDW intruded onto the continental shelf of the Amundsen Sea through the glacially scoured troughs in the seafloor (Jacobs et al., 2012; Turner et al., 2017). In the Amundsen Sea, the three major water masses are: (1) the relatively cold Antarctic Winter Water (WW), (2) the warmer and saltier CDW, and (3) a layer of seasonal Antarctic Surface Water (AASW).

2.2. Sampling

Seawaters from 37 sampling sites were collected from January 14th to February 3rd, 2016, during the R/V *Araon* Antarctic Amundsen Sea expedition (Fig. 1). Hydrographic surveys and seawater sampling were carried out in the Amundsen Sea using a conductivity-temperature-depth (CTD) and a rosette system holding 24 10 L-Niskin bottles (SeaBird Electronics, SBE 911 plus) aboard the Korean icebreaker R/V *Araon* during the ANA04B cruise (Fig. 1). The sampling sites encompassed 26 ice-free sites (red labels) in Amundsen Sea Polynya (ASP) and open sea (station 1), and 11 ice-covered sites (blue labels) on the ice shelf and along the sea ice zone (station 2).

Samples for the DOC analysis were drawn from the Niskin bottle by gravity filtration through an inline pre-combusted Whatman GF/F filter held in an acid-cleaned (0.1 M HCl) polycarbonate 47 mm filter holder (PP-47, ADVANTEC). The filter holder was attached directly to the Niskin bottle spigot. The filtrate (~250 mL) was collected in an acid-cleaned glass bottle after ~100 ml of seawater was passed through to clean the sampling system. The collected samples were distributed into two pre-combusted 20 ml glass ampoules with a sterilized serological pipette. Each ampoule was sealed with a torch, was quickly frozen, and preserved at −24 °C for further analyses in the land laboratory. Samples for inorganic nutrient analyses were pre-filtered in a manner similar to that for the DOC, transferred to a 50 ml conical tube, and immediately stored in a refrigerator at 2 °C prior to chemical analysis within ~1 month after filtration (GF/F).

2.3. Onboard analyses

The inorganic species, which include ammonium (NH_4^+), nitrate and nitrite ($NO_3^- + NO_2^-$), phosphate (PO_4^{3-}), and silicic acid ($Si(OH)_4$), were measured onboard within 3 days after sampling using a four-channel continuous Auto-Analyzer (QuAAtro, Seal Analytical) according to the Joint Global Ocean Flux Study (JGOFS) protocols described elsewhere (Sinha et al., 2007). The precision for NH_4^+, $NO_3^- + NO_2^-$, PO_4^{3-}, and $Si(OH)_4$ measurements were ± 0.18, ± 0.14, ± 0.02, and ± 0.28 μmol L^{-1}, respectively. The seawater samples for the chlorophyll *a* (chl-*a*) measurements were collected in the upper 100 m, and filtered onto 47 mm GF/F filters under low vacuum pressure. Chl-a was extracted from the filters with 90% acetone for 24 h (Parsons et al., 1984), and then measured onboard using a fluorometer (Trilogy, Turner Designs, USA).

2.4. DOC analyses

The DOC was measured using a Shimadzu TOC-L analyzer based on high temperature combustion. The Milli-Q water (blank) and the consensus reference material (CRM, 42–45 μM C for the DOC, deep Florida Strait water obtained from University of Miami) were measured every sixth analysis to check the accuracy of the measurements. Analytical errors based on the replicated measurements, which were at least three measurements per sample, were within 5% for the DOC.

2.5. UV–Vis and EEM measurements

Absorption spectra were obtained from 240 to 800 nm on a Shimadzu 1800 ultraviolet-visible (UV–Vis) spectrophotometer (Shimadzu Inc., Japan). The Napierian absorption coefficient a_λ reported below is calculated based on the equation: $a_\lambda = 2.303 \times$ optical density/pathlength. The 3D fluorescence EEMs were scanned using a Hitachi F-7000 luminescence spectrometer (Hitachi Inc., Japan) at the excitation/emission (Ex/Em) wavelengths of 250–500/280–550 nm. The excitation and the emission scans were set at 5 nm and 1 nm steps, respectively. Blank subtraction, inner filter effect correction, instrument correction, and Raman Unit normalization were performed. Identical integration times were used for water Raman scans and DOM samples. Further details on the EEM measurements and the procedures of the post-acquisition corrections are available in prior reports (Chen et al., 2010). The procedures for the Raman Unit (RU) normalization can be found in the literature (Lawaetz and Stedmon, 2009). PARAFAC modeling was performed using the MATLAB7.0.4 with a DOMFluor toolbox (Stedmon and Bro, 2008). All corrected EEMs of seawater ($n = 413$) were used for modeling. The number of components was determined

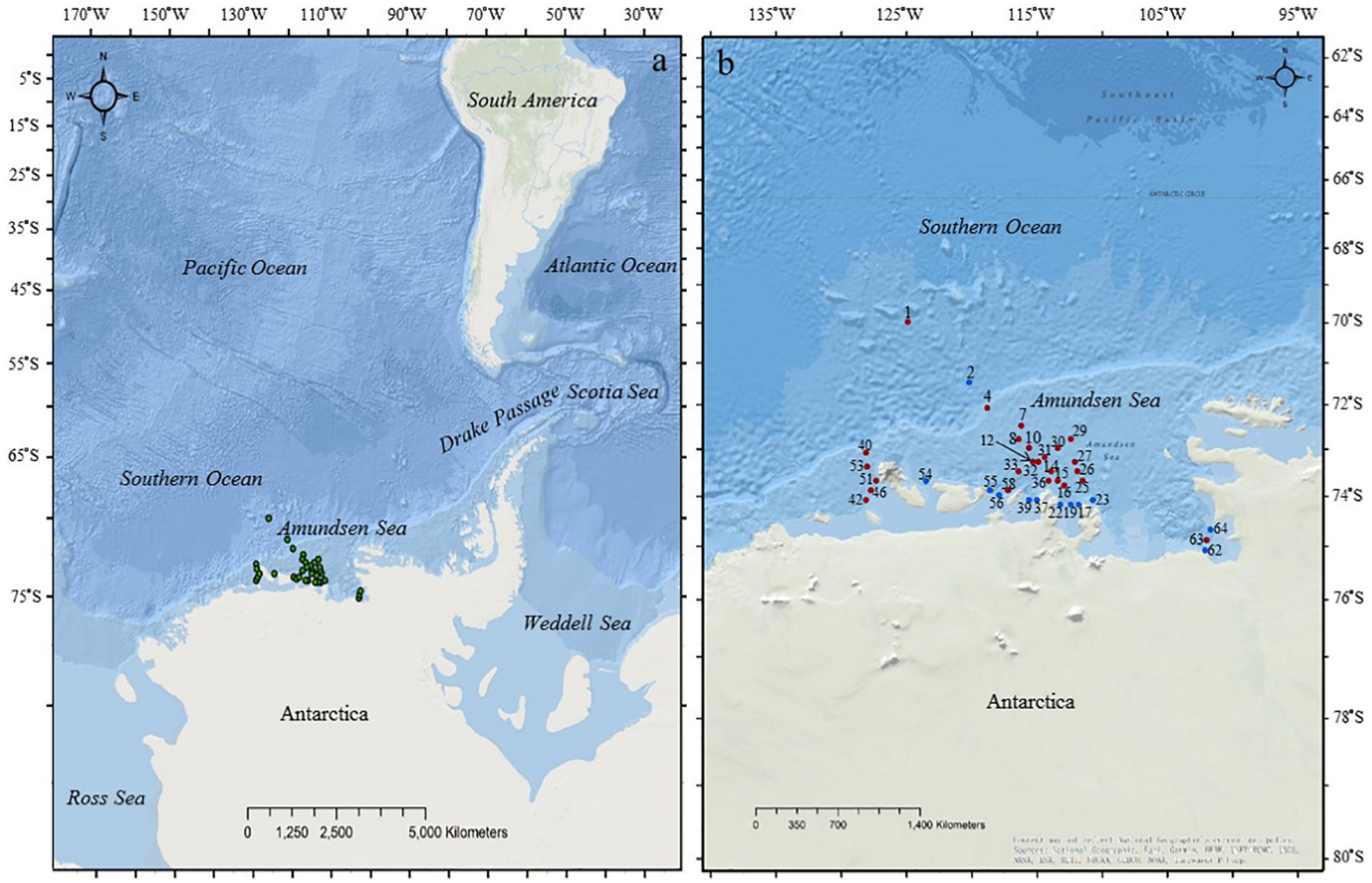

Fig. 1. Sampling sites in the Amundsen Sea, Antarctica (a-b). The ice-free and the ice-covered sites are marked with red and blue colors, respectively (b). (For interpretation of the references to colour in this figure legend, the reader is referred to the web version of this article.)

based on split-half validation. Biological index (BIX), which is an index of recent biological and autochthonous contribution, was calculated according to Huguet et al. (2009).

2.6. SEC-OCD and FT-ICR-MS measurements

SEC (chromatographic column: 250 × 20 mm, TSK, HW 50S; Toso, Japan) coupled with an OCD (DOC Labor Dr. Huber, Karlsruhe, Germany) was performed to measure the MW distribution for some samples (from stations 1, 8, 12, and 19) for surface seawaters (≤ 30 m,) and close-to-bottom seawaters. A volume (1 ml) of pre-filtered sample was injected directly into the instrument. A mobile phase containing a phosphate buffer of pH 6.85 (2.5 g KH_2PO_4 + 1.5 g $Na_2HPO_4 \times 2H_2O$ to 1 L MQ-H_2O, Merck) was used with a flow rate of 1.1 mL min^{-1}. A detailed configuration and method description of this system are available elsewhere (Huber et al., 2011; Chen et al., 2016a). We used typical molecular weight cutoffs for the fractions without calibration using standards.

FT-ICR-MS measurements were carried out with a 15-T FT-ICR-MS interfaced with an Apollo II electrospray ionization source (ESI, Bruker Daltonik, Germany) in negative ion mode. Due to the limited sample volume of each sample, we combined the samples from all the stations and depths from the ASP to obtain a sufficient volume for the FT-ICR-MS measurements (mixing in 1:1 volume ratio). The solid phase extraction (SPE) using BondElut cartridges (1 g PPL sorbent, Agilent Inc.) was performed prior to the FT-ICR-MS measurements as described elsewhere (Chen et al., 2016b). About 1 L of mixed acidified sample was discharged through the PPL cartridge. The cartridge was dried up completely with N_2 (> 99.999%) after all the samples passed through it. The adsorbed DOM on the cartridge was eluted with 6 ml of methanol into a pre-cleaned glass ampoule. The sample was injected with a Hamilton syringe with a flow rate of 2 µl min^{-1}. The negatively charged ions were accumulated in an argon-filled collision cell for 1 s and transferred to the ICR cell. A S/N ratio of ≥ 4 was set. The spectrum was evaluated in the mass range of *m/z* 200–650. Formulas were assigned using a Composer software (Sierra Analytics, Inc.) allowing the elemental combinations of $^{12}C_{0-\infty}{}^{1}H_{0-\infty}{}^{14}N_{0-5}{}^{32}S_{0-2}$. The mass accuracy threshold was set $\Delta m \leq \pm 1$ ppm. The following elemental ratio criteria were implemented: 2.2 > H/C > 0.3, O/C < 1.2. The double bond equivalent (DBE) rule and the nitrogen rule were applied with ambiguous formulas rechecked with the "chemical building block" approach and intrinsic stable isotope ^{13}C (Schaub et al., 2005; Koch et al., 2007). DBE and modified aromatic index (AI_m) were calculated based on the formula: DBE = 1 + 1/2(2C–H + N) and AI_m = (1 + C-0.5O-S-0.5H)/(C-0.5O-S-N-P), respectively (Koch et al., 2005; Koch and Dittmar, 2006).

2.7. Estimation of Net DOC production ratio (NDPr)

The Net DOC production ratio (NDPr) was based on the ratio of ΔDOC/NCP. DOC accumulation (ΔDOC) in the marine surface was estimated with the differences in the observed concentrations of DOC between the surface waters and the underlying waters at a depth of 100 m (a depth below the euphotic zone, Eq. (1)) as used in a recent report in the Southern Atlantic Ocean (Romera-Castillo et al., 2016). The reduction of nitrate and nitrite concentrations due to photosynthetic drawdown were similarly estimated and were utilized to estimate NCP (Eqs. (2)–(3)). It is based on two assumptions: (1) the water column is well-mixed during the winter overturn, and (2) water at a depth of 100 m maintains pre-bloom wintertime conditions. The

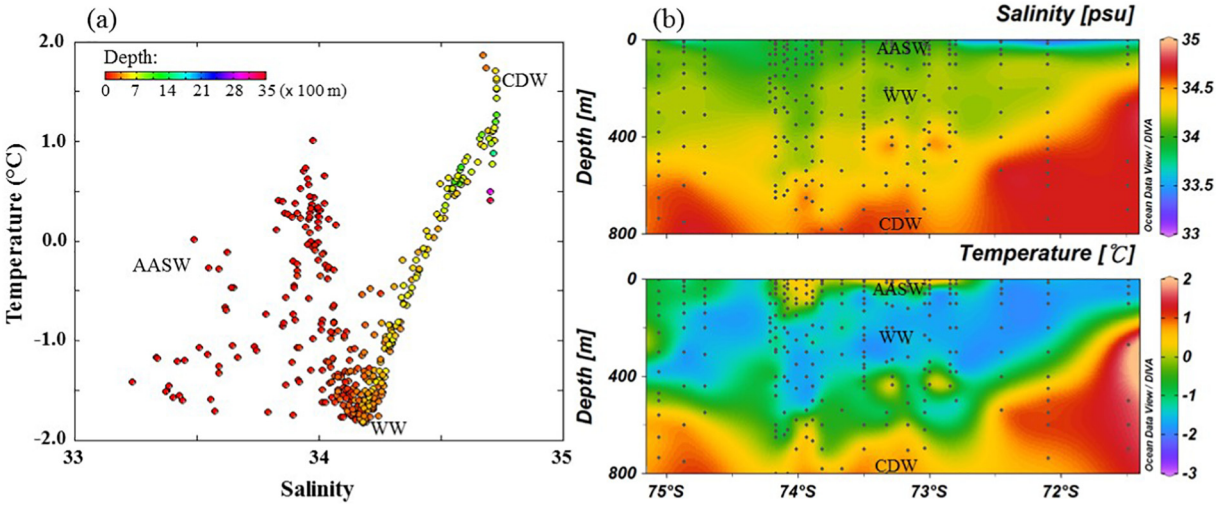

Fig. 2. Property-property plot of θ-S (a) and section plots of salinity and temperature (b) of all seawater samples. The water mass types identified include: Antarctic Surface Water (AASW), Winter Water (WW), and Circumpolar Deep Water (CDW) in the Amundsen Sea, Antarctica. Note that station 1 is excluded from the ODV plots for proper extrapolation purpose. Plot (b) was produced with an Ocean Data View.

ecological stoichiometry of C and N was utilized for the estimation of NDPr. The related equations are below:

$$\Delta DOM = DOM_{surface} - DOM_{100\,m} \quad (1)$$

$$\Delta nutrient = nutrient_{100\,m} - nutrient_{surface} \quad (2)$$

$$NDPr = \Delta DOC/NCP = \Delta DOC/(6.6 \times \Delta NO_x^-) \times 100\% \quad (3)$$

where 6.6 is the molar conversion from N to C units and $\Delta NO_x^- = \Delta(NO_3^- + NO_2^-)$ (Redfield, 1958).

3. Results and discussion

3.1. DOC accumulation, CDOM exhaustion, and nutrients drawdown at surface ocean

As seen from Fig. 2, the intrusion of the relatively warm CDW to the ASP at a depth of ~400 m in the ASP and a much shallower depth in the open sea area can be seen in the section plots of salinity and temperature, which was in line with a previous report of CDW intrusion channeled through the Dotson-Getz Trough in the study area (Turner et al., 2017). From the chl-*a* (up to ~11 mg m^{-3}) data of the current work as compared with those in a previous report of > 20 mg m^{-3} based on the samples collected from mid-December 2010, to early January 2011, the sampling time (from mid-January to early February 2016) from this study seems to fall into a declining period of phytoplankton bloom (Fig. 3).

From the latitudinal section plots of the DOM accumulation relative to the depth at 100 m based on Eq. (1) (ΔDOM, Fig. 3), the ΔDOC values reached the maxima (~19.2 μM) at the surface (~10 m depth) of station 31, which roughly corresponds to the center of the ASP and above the Dotson-Getz Trough. In contrast, the accumulation of absorption coefficients, Δa_{254} and Δa_{350}, were the lowest as shown by the net negative accumulation values of roughly $-9.7\,m^{-1}$ for a_{254} and $-9.5\,m^{-1}$ for a_{350} at the top surface (0 m depth) in the same location. However, the highest absolute levels (up to $14.0\,m^{-1}$ for a_{254} and $12.3\,m^{-1}$ for a_{350}) were seen at a depth of ~30 m. The results suggest a highly photo- and/or bio-labile nature of freshly produced CDOM. Meanwhile, the nutrient drawdown of ΔNO_x^-, ΔPO_4^{3-}, and $\Delta Si(OH)_4$ based on Eq. (3) was obvious in the ASP with the maximum values of ~16 μM, ~1 μM, and ~10 μM, respectively (Fig. 3). The ratios of ΔNO_x^-: ΔPO_4^{3-} were ~16, which were in line with a previous report of the nutrient drawdown ratio for *Phaeocystis antarctica* (up to 90% in the ASP) observed in the neighboring Ross Sea (Arrigo et al., 1999).

3.2. Dominance of low molecular weight DOC at the surface ocean in the polynya

The representative SEC-OCD results revealed noticeable discrepancies in the molecular distributions of the DOM at different stations and depths (Fig. 4, Table S3). The surface waters (< 30 m to the surface) in the highly productive ASP showed the dominance of low molecular weight neutrals fraction (80%) with a nominal average molecular weight M_n of < ~350 Da (Huber et al., 2011), whereas station 1 in the open ocean area did not present this feature (Fig. 4b). Moreover, the comparison of the SEC-OCD data for the surface seawaters (≤ 30 m to surface) versus the close-to-seafloor seawaters (≤ 30 m from bottom) illustrated a sharp contrast between the prominent low molecular weight fractions at surface waters in the ASP and their less pronounced presence in the deeper waters (Fig. 4a). It is noteworthy that deep water in the Southern Ocean is primarily controlled by distant (i.e., allochthonous) processes and thus that the DOM composition might have been changed for the close-to-bottom waters (Bercovici and Hansell, 2016). Interestingly, the SEC-OCD results at the ice-free sites in ASP in the present study were similar to those observed in the ice-covered sites of the Chukchi Sea in the Arctic Ocean (Chen et al., 2018). The ice-free sites in ASP are dominated by *Phaeocystis antarctica*, while the ice-covered sites in the Chukchi Sea are prevailed by *Phaeocystis pouchetii* during under-ice phytoplankton bloom (Lee et al., 2016; Assmy et al., 2017). The coincidence may suggest there is a link between the productions of low molecular weight DOM by these two kinds of phytoplankton taxa in polar environments.

3.3. Massive labile CDOM production

The sampling stations were categorized into ice-free and ice-covered (> 15% coverage) sites to assess the potential effects of the ongoing sea ice and the ice shelf retreat. The depth profile of CDOM showed wide variability among stations and depth, spiked at the surface of center station 31 of the ASP and implied the CDOM production in ocean surface (Fig. S1). The DOC concentrations were 43 ± 8 μM and 41 ± 4 μM for the ice-free and the ice-covered sites, respectively (Table S1, Fig. S1). These values are generally comparable to those in prior reports (Table S2). However, the CDOM was very high in this study. The absorption coefficients of a_{254} were 2.4 ± 2.7 m^{-1} and 2.6 ± 2.9 m^{-1} for the ice-free and the ice-covered sites, respectively. The a_{350} values were 1.2 ± 2.5 m^{-1} and 1.3 ± 2.8 m^{-1} for the ice-free and the ice-covered sites, respectively. The a_{355} averaged 1.2 m^{-1},

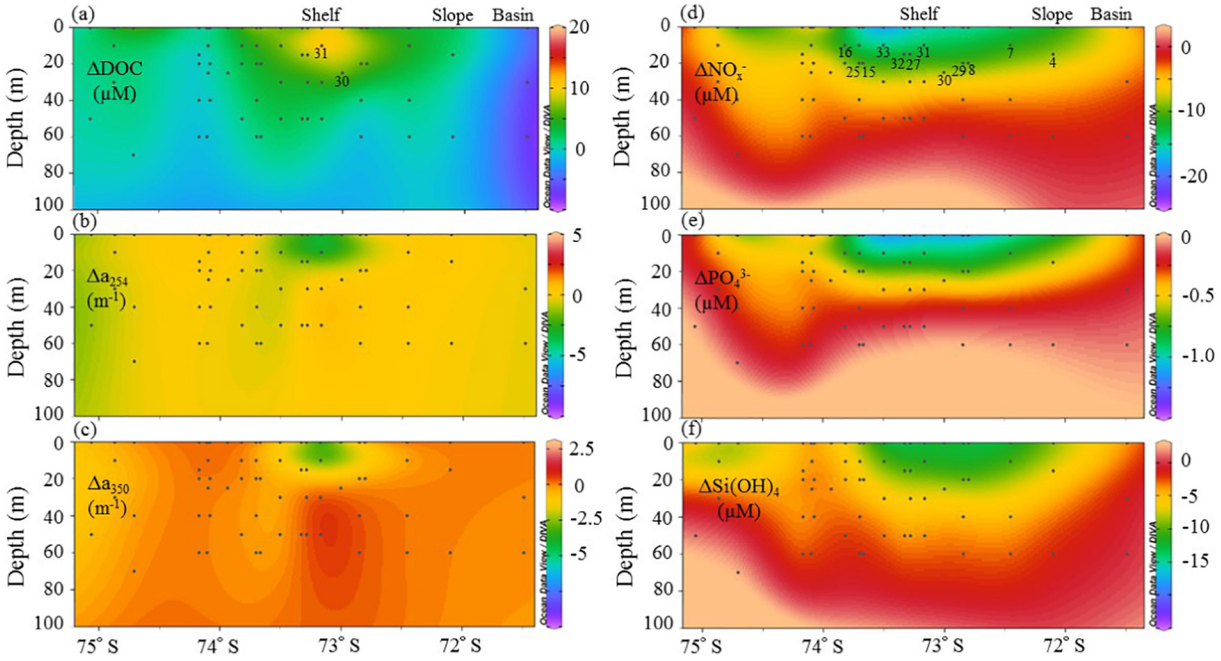

Fig. 3. DOC accumulation (a), CDOM degradation (b-c), and nutrients drawdown (d-f) at the ocean surface of the Amundsen Sea Polynya. The labeled numbers are stations. Station 31 is approximately at the center of the Amundsen Sea Polynya. $NO_x^- = NO_3^- + NO_2^-$.

which was about one order of magnitude higher than those reported in other Antarctic seas, such as the Ross Sea, the Weddell Sea, and the East Antarctica. The values were also ~2–3 times higher than those reported in the Amundsen Sea and the neighboring Bellingshausen Sea, which were sampled primarily in February other than mid-January to early February in this study.

The observation may be linked to the biogeneration of the CDOM reported in the peninsular region and the Amundsen Sea Polynya of the Southern Ocean (Ortega-Retuerta et al., 2009; Lee et al., 2016). Considering that the peak of the phytoplankton bloom occurs in January

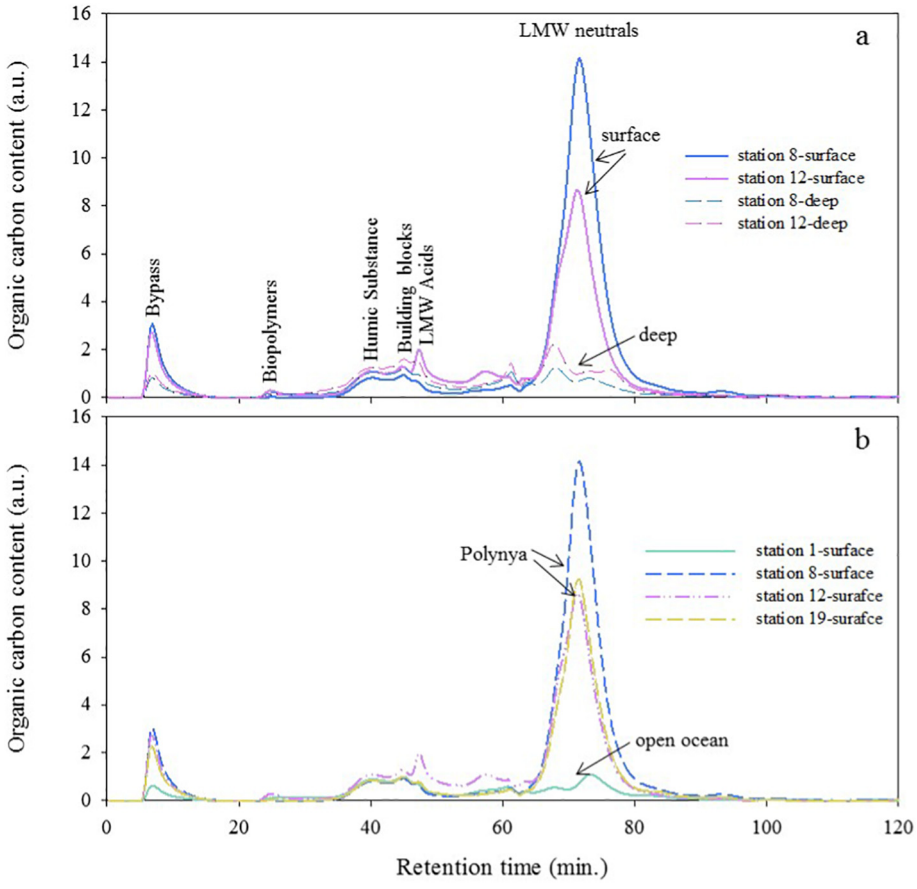

Fig. 4. SEC-OCD chromatograms of the surface (≤ 30 m) and the close-to-seafloor seawater samples from the Amundsen Sea of the Southern Ocean. (a) Comparison between surface and deep waters, (b) Comparison between Polynya and open ocean waters. Typical molecular weight cutoffs for the fractions: Biopolymers (M_n > 10 kDa); Humic substances (M_n = ~1 kDa); Building blocks (M_n = 350–500 Da); LMW acids = Low molecular weight acids (M_n < 350 Da); LMW neutrals (M_n < 350 Da). M_n represents nominal average molecular weight ($M_n = \Sigma N_i M_i / \Sigma N_i$, where M is the molecular mass and N is the number of molecules). Bypass was to obtain a detector signal at the dead volume time of each run. Deep water depth: ~500 m and 800 m at station 8 and 12, respectively.

Table 1
Estimation of DOM accumulation (ΔDOM), nutrients drawdown, and net DOC production ratio (NDPr) in surface waters at ice-free sites of the Amundsen Sea Polynya in austral summer.

Parameter	Δa_{254}	Δa_{350}	ΔNO_x-	ΔDOC	NDPr (%)	NDPr (%)
Unit	m^{-1}	m^{-1}	μM	μM	this study	Global oceans
Amundsen Sea	−0.2	−0.2	9.4 ± 4.3	4.6 ± 3.4	9 ± 6	17

$\Delta DOM = DOM_{surface} - DOM_{100\ m}$ (Eq. (1)); $\Delta nutrient = nutrient_{100\ m} - nutrient_{surface}$ (Eq. (2)).
Net DOC production ratio (NDPr) = $\Delta DOC/(6.6 \times \Delta NO_3^-)$ (Eq. (3)). 6.6 is the molar conversion from N to C units.
$NO_x- = NO_3- + NO_2-$.

(Yager et al., 2016), it is reasonable that the CDOM found in this study with samples collected from mid-January to early February is higher than those observed from February (Lee et al., 2016). Despite the massive CDOM production observed, the $-0.2\ m^{-1}$ net negative surface accumulation of the absorption coefficients of a_{254} and a_{350} indicated the photo- and/or bio-labile nature of the freshly produced CDOM at the ocean surface (Table 1, Fig. 3). The high reactivity of CDOM may contribute to the low accumulation of semilabile DOC at the surface. More discussion on the semilabile DOC dynamics is presented in Section 3.5.

3.4. High tyrosine-like fluorescence $C_{270/306}$ and a potential glacier-born component $C_{300/342}$

The tyrosine-like fluorescence component, $C_{270/306}$, was as high as 0.3 RU, one order of magnitude higher than that observed in the Weddell Sea of Antarctica in the austral winter (Fig. 5) (Stedmon et al., 2011). In the Antarctic seas, there was only one report about fluorescent DOM (FDOM) in the Weddell Sea. Protein-like fluorescence has been suggested to be heterogeneous in some ecosystems. It is associated with both proteinaceous materials and phenolic moieties in a coastal wetland ecosystem (Maie et al., 2007). Tyrosine- and tryptophan-like fluorescence has been observed to be correlated to the total hydrolysable amino acids (THAA) in a coastal to oceanic environment, suggesting its usefulness to trace the dynamics of THAA (Yamashita and Tanoue, 2003). The tyrosine-like component here presumably is not phenolic moieties considering the Amundsen Sea is remote from terrestrial DOM sources (Maie et al., 2007; Rosario-Ortiz and Korak, 2017). Its high abundance is consistent with the high protein production (~60.0% of overall photosynthetic carbon allocation) of phytoplankton in the Amundsen Sea compared to the lower protein production (7–23%) reported previously in other seas in the Southern Ocean, which include the McMurdo Sound, the East Antarctica, and the Weddell Sea (Song et al., 2016). Interestingly, the component $C_{300/342}$ is similar to a $C_{305/344}$ fluorescence observed in Arctic Ocean while it is not usually seen in subtropical or temperate aquatic ecosystems, suggesting a potential to trace glacier DOM source (Chen et al., 2010, 2018).

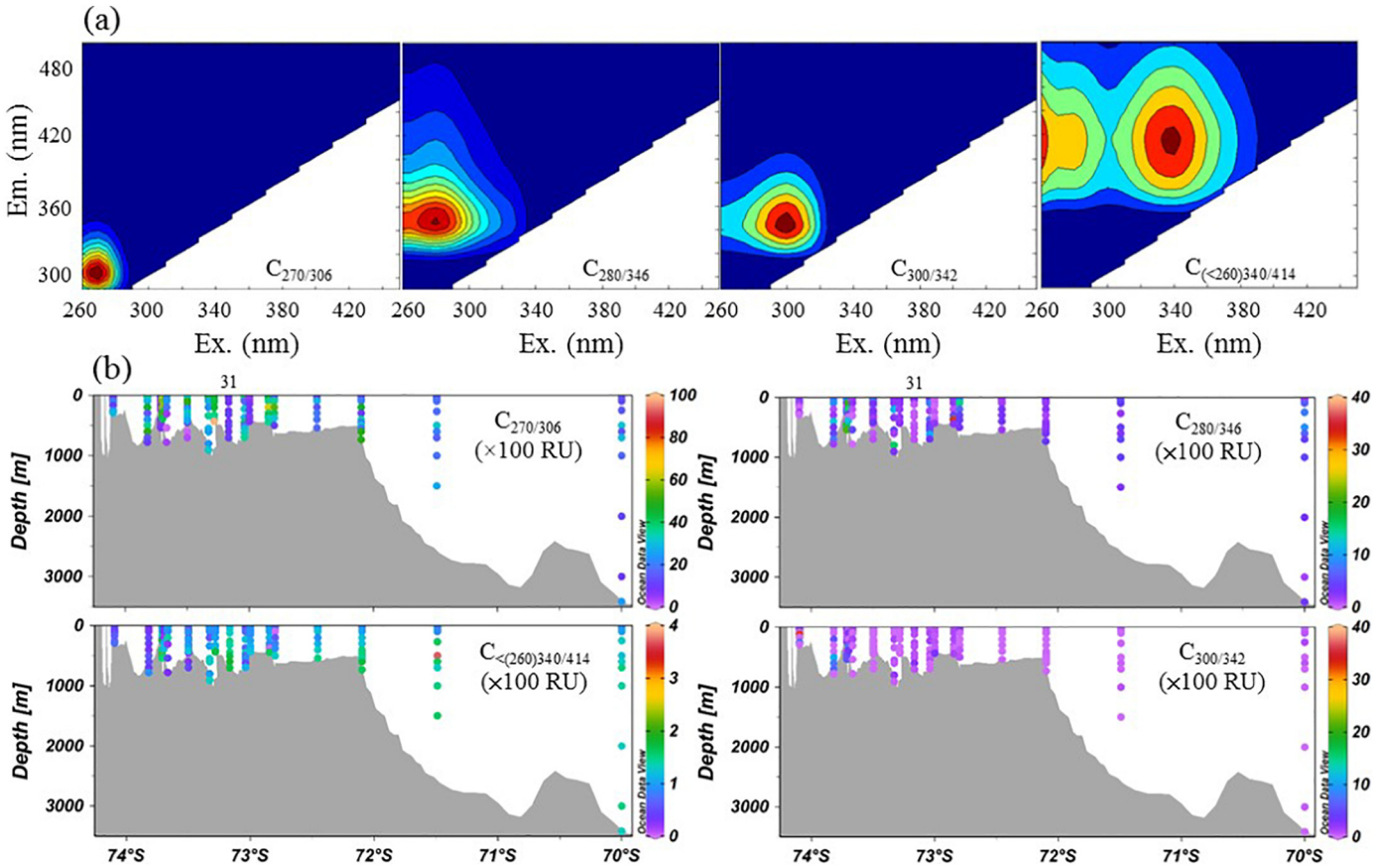

Fig. 5. Contour plots of identified four EEM-PARAFAC components (a) and depth profile of the components (b) for seawaters in the Amundsen See. The labeled station 31 is approximately at the center of the Amundsen Sea Polynya.

3.5. Low surface accumulation of semilabile DOC in the Amundsen Sea Polynya

The net DOC production ratios (NDPr) in the surface waters were estimated using Eq. (3) only for the ice-free sites since no accumulation was observed at the ice-covered sites. This ratio can indicate the surface accumulation and vertical downward export efficiency of the DOC from the photic surface oceans to the deep non-photic zone, which strongly depends on the DOM bioavailability and the physical oceanographic conditions, such as the currents. The average ΔDOC and ΔNO_x^- were 4.6 ± 3.3 μM and 9.4 ± 4.3 μM, respectively, among the sites (Table 1). The estimated NDPr was 9 ± 6%, which was lower than the global trend of the NDPr level (i.e., 17%, Hansell and Carlson, 1998; Romera-Castillo et al., 2016). However, low surface accumulation of DOC in the Ross Sea of Antarctica (as low as 4% out of cumulative primary productivity over the course of bloom) was also observed during spring phytoplankton bloom (Carlson et al., 1998).

The low surface accumulation of the DOC can be explained by several scenarios: (1) an eutrophic ecosystem, (2) a bio-labile nature of freshly produced DOM in the surface ocean, (3) its photo-labile nature, and (4) its longer residence time in the surface of the ocean due to the low density of foam-like *Phaeocystis antarctica*. It is suggested that DOC accumulation has been linked to nutrient depletion and the nonlimiting nutrients in the Antarctic waters offer some explanation of low surface DOC accumulation (Ittekkot et al., 1981; Carlson et al., 1998). As stated above, a net negative accumulation of absorption coefficients a_{254} and a_{350} at the surface of the ocean indicates the labile nature of the massively produced CDOM. In fact, a high bioavailability of DOM in the upper water column and a low benthic respiration have been previously reported in the ASP (Ducklow et al., 2015; Sipler and Connelly, 2015; Kim et al., 2016). The relatively high abundance of ~4% of peptides compounds (Table S4, Fig. 6) observed from the FT-ICR-MS data also matched with the bio-labile peptides in the DOM, despite the fact that PPL solid phase extraction can bias against the heteroatomic compounds and peptides (Chen et al., 2016c). The potentially high reactivity of DOM can also be supported by the composition of the molecular formulas of 41% CHON compounds (including peptides, amines, amides, etc.), 28% CHOS compounds (including S-containing peptides, thiols, sulfonic acids, etc.), 13% aliphatics, and 38% of highly unsaturated with high oxygen compounds (O/C > 0.5), which are often found to be relatively labile in the aquatic ecosystems (Singer et al., 2012; Chen et al., 2016b; Wang et al., 2018). As mentioned above, this sample comes from a composite sample from all stations and depth. Thus, the abundance of bio-labile compound types could be even higher in surface waters. A previous study reported a cryophilic heterotrophic microbial community became more active during the *Phaeocystis antarctica* bloom in the ASP (Williams et al., 2016). Prior studies on other Antarctic shelves, such as the Ross Sea and the Weddell Sea, suggested that the DOC produced during the phytoplankton bloom is rather bio-labile within its production season with a majority was consumed by bacterioplankton within 19 days (Kähler et al., 1997; Carlson et al., 1998). Large mineralization of amino acids to NH_4^+ was observed in Antarctic coastal waters previously (Tupas et al., 1994). Even in austral winter, biological hot spots exist in Antarctic waters (Shen et al., 2017). The bio-lability of Antarctic DOM lend support to the relatively low accumulation of DOC. Furthermore, the photo-labile nature of the CDOM is supported by the depth profile of the CDOM accumulation at the surface of the ocean in this study (Fig. 3). The CDOM displayed a net negative accumulation at the depths of ~0–20 m at the ASP center station 31 in contrast with its highest absolute levels at a depth of ~30 m, which implies the simultaneous operation of photo- and bio-degradation to cause the rapid decay of the CDOM at the ocean surface to a depth ~20 m. There is a well-known ozone hole above Antarctica which may lead to strong solar radiation despite of high latitude. In addition, the predominant phytoplankton taxa of *Phaeocystis antarctica* have foam-like structures without the silicon shell as in diatoms that have a much faster settling rate (0–0.19 m d^{-1} vs. > 100 m d^{-1}, Alldredge and Gotschalk, 1989; Becquevort and Smith Jr, 2001). With the low settling rate of 0–0.19 m d^{-1}, it would take at least hundreds of days for the *Phaeocystis antarctica* debris to reach a depth of 100 m. The longer residing debris can lead to less DOM export since the particulate organic matter (POM) is a standing stock of DOM. Undoubtedly, it is probable that phytoplankton debris adheres to particles with a higher density and settles faster in this case. Meanwhile, the longer residence time in the upper water column could promote photo- and bio-degradation before the phytoplankton debris is transported to depth. Off-shelf flushing was postulated as the main reason for low vertical export of the particulate organic carbon in the ASP in a prior report (Lee et al., 2017). Unlike other Antarctic seas, there is no bottom water formation caused by the CDW intrusion on the shelf of the ASP. However, the off-shelf flushing should be of little importance to surface waters over the timescale of a few months and considering the similar low accumulation in the neighboring Ross Sea where there is bottom water formation.

It is not clear whether this low surface accumulation persists until winter or during other non-phytoplankton bloom seasons. There is a possibility that this low molecular weight-dominated, heteroatomic-enriched, and high tyrosine-like fluorescence DOM freshly produced by the *Phaeocystis antarctica* might be particularly labile. The situation might not be the same for the off-phytoplankton bloom season when the dominant phytoplankton community shifts and the environmental factors are different, such as light availability, microbial activity, and the atmospheric and oceanic forcing. For example, diatoms were observed to be dominant in the non-bloom waters in the ASP (Schofield et al., 2015). Moreover, substantial differences in the export efficiency of the particles were previously reported even during the early and mid-bloom vs. the high bloom periods (Yager et al., 2016), which implies temporal variations of the POM export. Hence, the export pattern of the DOM can also be affected by the changes in the POM export because of the dynamic exchanges between the POM and DOM (He et al., 2016).

4. Summary and conclusions

This study shows several significant findings regarding the DOM dynamics in a highly productive Antarctic sea, which are the massive production of low molecular weight DOC, the labile CDOM, the high tyrosine-like component, and the low surface accumulation of the DOC during a summer phytoplankton bloom in a highly productive Antarctic sea intruded by warm CDW channeled through cross-shelf troughs. In addition, because of the higher DOC at ice-free versus ice-covered sites, and the weak but significant positive correlations of photosynthetically active radiation (PAR) with chl-*a* and DOC, primary productivity and DOC enhancement could potentially be accelerated with the ice retreat and elevated light availability. In contrast, the CDOM and FDOM seem to be rather insusceptible to the change of ice-cover. Most importantly, the low surface accumulation and thus low downward export and advection of low molecular weight DOC in this highly productive Antarctic sea should be considered in the future estimates of global carbon exports as a potential fast turnover of DOC, which is hinted by the labile nature of the massively produced CDOM. At this point, we cannot confirm yet the interlink between the low molecular weight DOM characteristics and the low accumulation of semilabile DOC at surface ocean and its subsequent export. More field data in wide ranges of areas and different seasons are essential to allow an accurate estimation of the fraction of DOM sequestered in the deep ocean under a changing climate.

Conflicts of interest

The authors declare no conflict of interest.

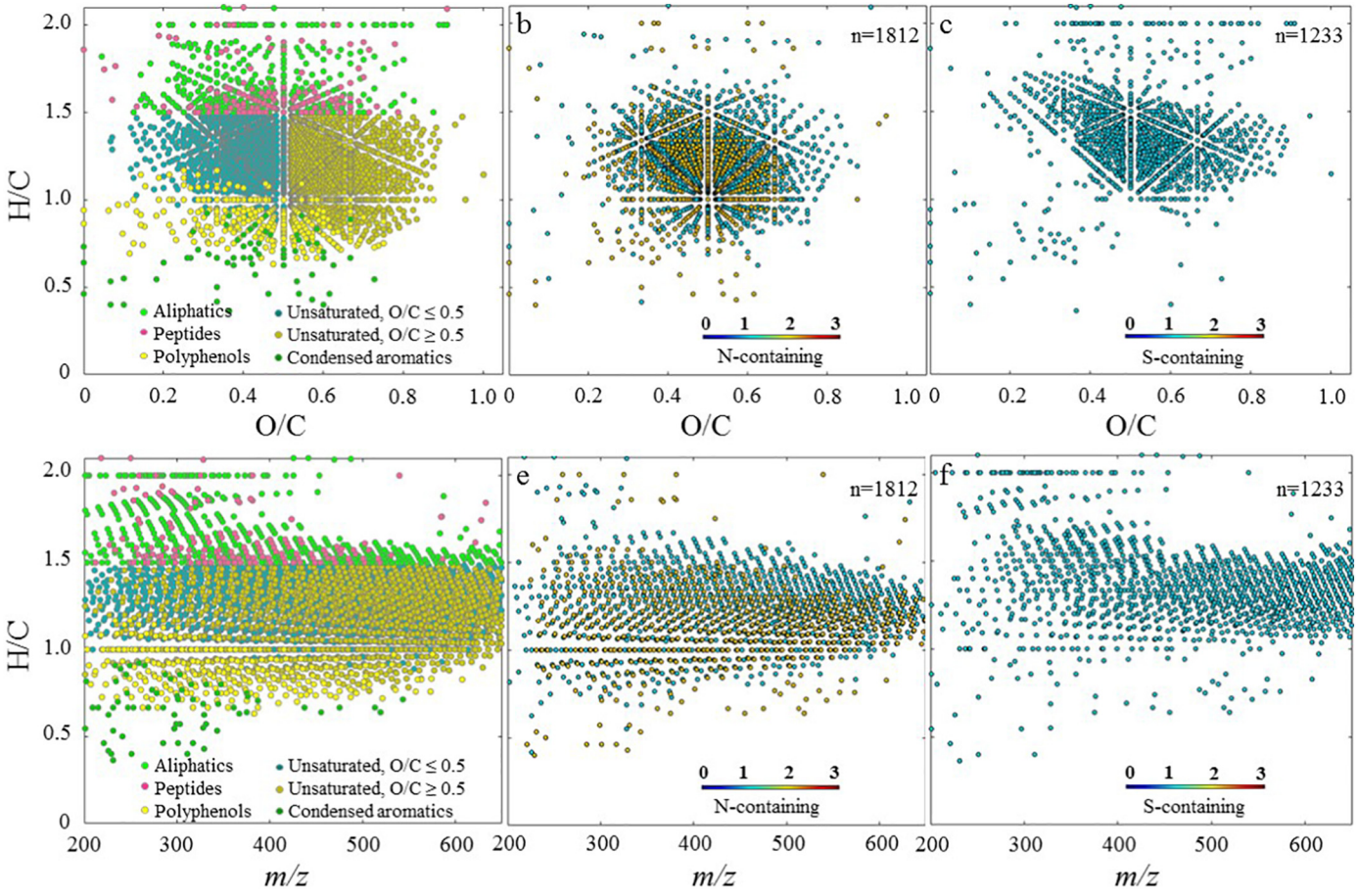

Fig. 6. Van Krevelen diagrams (a-c) and H/C vs. *m/z* plots (d-f) of the formula distribution for the seawater sample from the Amundsen Sea Polynya. N- and S-containing formula account for 41% and 28% of the total identified formula, respectively. Compounds are categorized as follows (Spencer et al., 2014): Aliphatics (13%): O/C < 0.9, H/C > 1.5, $N = 0$; Peptides (4%): O/C < 0.9, H/C > 1.5, $N > 0$; Highly unsaturated with low oxygen (37%): $AI_m < 0.5$, H/C < 1.5, O/C ≤ 0.5; Highly unsaturated with high oxygen (38%): $AI_m < 0.5$, H/C < 1.5, O/C > 0.5; Polyphenols (7%): $0.67 > AI_m > 0.5$; Condensed aromatics (1%): $AI_m \geq 0.67$.

Acknowledgements

This work was supported by the National Research Foundation of Korea (NRF) grant funded by the Korea Government (MSIP) (No. 2017R1A4A1015393) and the Korea Polar Research Institute project (PE18060). The authors thank the captain and crew of the R/V *Araon* for help with sampling during the Antarctic Amundsen Sea expedition. Thanks go to Dr. Youhei Yamashita for helpful discussion. The authors also thank Dr. Ronald Benner for his insightful comments. Special thanks go to Dr. Boris Peter Koch for his comments and help with the FT-ICR-MS data re-calibration.

Appendix A. Supplementary data

Supplementary data to this article can be found online at https://doi.org/10.1016/j.marchem.2019.04.009.

References

Alderkamp, A.-C., van Dijken, G.L., Lowry, K.E., Connelly, T.L., Lagerström, M., Sherrell, R.M., Haskins, C., Rogalsky, E., Schofield, O., Stammerjohn, S.E., Yager, P.L., Arrigo, K.R., 2015. Fe availability drives phytoplankton photosynthesis rates during spring bloom in the Amundsen Sea Polynya, Antarctica. Elem. Sci. Anth. 3, 000043.

Alldredge, A.L., Gotschalk, C.C., 1989. Direct observations of the mass flocculation of diatom blooms: characteristics, settling velocities and formation of diatom aggregates. Deep Sea Res. A. 36, 159–171.

Arrigo, K.R., van Dijken, G.L., 2003. Phytoplankton dynamics within 37 Antarctic coastal polynya systems. J. Geophys. Res. Oceans 108, 3271.

Arrigo, K.R., van Dijken, G., Long, M., 2008. Coastal Southern Ocean: a strong anthropogenic CO_2 sink. Geophys. Res. Lett. 35, L21602.

Arrigo, K.R., Robinson, D.H., Worthen, D.L., Dunbar, R.B., DiTullio, G.R., VanWoert, M., Lizotte, M.P., 1999. Phytoplankton community structure and the drawdown of nutrients and CO_2 in the Southern Ocean. Science 283, 365–367.

Assmy, P., Fernández-Méndez, M., Duarte, P., Meyer, A., Randelhoff, A., Mundy, C.J., Olsen, L.M., Kauko, H.M., Bailey, A., Chierici, M., Cohen, L., Doulgeris, A.P., Ehn, J.K., Fransson, A., Gerland, S., Hop, H., Hudson, S.R., Hughes, N., Itkin, P., Johnsen, G., King, J.A., Koch, B.P., Koenig, Z., Kwasniewski, S., Laney, S.R., Nicolaus, M., Pavlov, A.K., Polashenski, C.M., Provost, C., Rösel, A., Sandbu, M., Spreen, G., Smedsrud, L.H., Sundfjord, A., Taskjelle, T., Tatarek, A., Wiktor, J., Wagner, P.M., Wold, A., Steen, H., Granskog, M.A., 2017. Leads in Arctic pack ice enable early phytoplankton blooms below snow-covered sea ice. Sci. Rep. 7, 40850.

Becquevort, S., Smith Jr., W.O., 2001. Aggregation, sedimentation and biodegradability of phytoplankton-derived material during spring in the Ross Sea, Antarctica. Deep-Sea Res. II 48, 4155–4178.

Bercovici, S.K., Hansell, D.A., 2016. Dissolved organic carbon in the deep Southern Ocean: local versus distant controls. Glob. Biogeochem. Cycles 30, 350–360.

Carlson, C.A., Ducklow, H.W., Hansell, D.A., Smith, W.O., 1998. Organic carbon partitioning during spring phytoplankton blooms in the Ross Sea polynya and the Sargasso Sea. Limnol. Oceanogr. 43 (3), 375–386.

Chen, M.L., Price, R.M., Yamashita, Y., Jaffé, R., 2010. Comparative study of dissolved organic matter from groundwater and surface water in the Florida coastal Everglades using multi-dimensional spectrofluorometry combined with multivariate statistics. Appl. Geochem. 25, 872–880.

Chen, M., He, W., Choi, I., Hur, J., 2016a. Tracking the monthly changes of dissolved organic matter composition in a newly constructed reservoir and its tributaries during the initial impounding period. Environ. Sci. Pollut. Res. 23, 1274–1283.

Chen, M., Kim, S., Park, J.-E., Kim, H., Hur, J., 2016b. Effects of dissolved organic matter (DOM) sources and nature of solid extraction sorbent on recoverable DOM composition: implication into potential lability of different compound groups. Anal. Bioanal. Chem. 408, 4809–4819.

Chen, M., Kim, S., Park, J.-E., Jung, H.-J., Hur, J., 2016c. Structural and compositional changes of dissolved organic matter upon solid-phase extraction tracked by multiple analytical tools. Anal. Bioanal. Chem. 408 (23), 6249–6258.

Chen, M., Jung, J., Lee, Y.K., Hur, J., 2018. Surface accumulation of low molecular weight

dissolved organic matter in surface waters and horizontal off-shelf spreading of nutrients and humic-like fluorescence in the Chukchi Sea of the Arctic Ocean. Sci. Total Environ. 639, 624–632.
Ducklow, H.W., Wilson, S.E., Post, A.F., Stammerjohn, S.E., Erickson, M., Lee, S., Lowry, K.E., Sherrell, R.M., Yager, P.L., 2015. Particle flux on the continental shelf in the Amundsen Sea Polynya and Western Antarctic peninsula. Elem. Sci. Anth. 3, 000046.
Fretwell, P., Pritchard, H.D., Vaughan, D.G., Bamber, J.L., Barrand, N.E., Bell, R., Bianchi, C., Bingham, R.G., Blankenship, D.D., Casassa, G., Catania, G., Callens, D., Conway, H., Cook, A.J., Corr, H.F.J., Damaske, D., Damm, V., Ferraccioli, F., Forsberg, R., Fujita, S., Gim, Y., Gogineni, P., Griggs, J.A., Hindmarsh, R.C.A., Holmlund, P., Holt, J.W., Jacobel, R.W., Jenkins, A., Jokat, W., Jordan, T., King, E.C., Kohler, J., Krabill, W., Riger-Kusk, M., Langley, K.A., Leitchenkov, G., Leuschen, C., Luyendyk, B.P., Matsuoka, K., Mouginot, J., Nitsche, F.O., Nogi, Y., Nost, O.A., Popov, S.V., Rignot, E., Rippin, D.M., Rivera, A., Roberts, J., Ross, N., Siegert, M.J., Smith, A.M., Steinhage, D., Studinger, M., Sun, B., Tinto, B.K., Welch, B.C., Wilson, D., Young, D.A., Xiangbin, C., Zirizzotti, A., 2013. Bedmap2: improved ice bed, surface and thickness datasets for Antarctica. Cryosphere 7, 375–393.
Hansell, D.A., Carlson, C.A., 1998. Net community production of dissolved organic carbon. Glob. Biogeochem. Cycles 12, 443–453.
He, W., Chen, M., Schlautman, M.A., Hur, J., 2016. Dynamic exchanges between DOM and POM pools in coastal and inland aquatic ecosystems: a review. Sci. Total Environ. 551–552, 415–428.
Huber, S.A., Balz, A., Abert, M., Pronk, W., 2011. Characterisation of aquatic humic and non-humic matter with size-exclusion chromatography – organic carbon detection – organic nitrogen detection (LC-OCD-OND). Water Res. 45, 879–885.
Huguet, A., Vacher, L., Relexans, S., Saubusse, S., Froidefond, J.M., Parlanti, E., 2009. Properties of fluorescent dissolved organic matter in the Gironde Estuary. Org. Geochem. 40, 706–719.
Ittekkot, V., Brockmann, U., Michaelis, W., Degens, E.T., 1981. Dissolved free and combined carbohydrates during a phytoplankton bloom in the northern North-Sea. Mar. Ecol. Prog. Ser. 4 (3), 299–305.
Jacobs, S., Jenkins, A., Hellmer, H., Giulivi, C., Nitsche, F., Huber, B., Guerrero, R., 2012. The Amundsen Sea and the Antarctic Ice Sheet. Oceanography 25, 154–162.
Kähler, P., Bjornsen, P.K., Lochte, K., Antia, A., 1997. Dissolved organic matter and its utilization by bacteria during spring in the Southern Ocean. Deep-Sea Res. II 44, 341–353.
Kim, S.-H., Choi, A., Jin Yang, E., Lee, S., Hyun, J.-H., 2016. Low benthic respiration and nutrient flux at the highly productive Amundsen Sea Polynya, Antarctica. Deep-Sea Res. II 123, 92–101.
Koch, B.P., Dittmar, T., 2006. From mass to structure: an aromaticity index for high-resolution mass data of natural organic matter. Rapid Commun. Mass Spectrom. 20, 926–932.
Koch, B.P., Witt, M., Engbrodt, R., Dittmar, T., Kattner, G., 2005. Molecular formulae of marine and terrigenous dissolved organic matter detected by electrospray ionization Fourier transform ion cyclotron resonance mass spectrometry. Geochim. Cosmochim. Acta 69, 3299–3308.
Koch, B.P., Dittmar, T., Witt, M., Kattner, G., 2007. Fundamentals of molecular formula assignment to ultrahigh resolution mass data of natural organic matter. Anal. Chem. 79 (4), 1758–1763.
Lawaetz, A.J., Stedmon, C.A., 2009. Fluorescence intensity calibration using the Raman scatter peak of water. Appl. Spectrosc. 63, 936–940.
Lee, Y.C., Park, M.O., Jung, J., Yang, E.J., Lee, S.H., 2016. Taxonomic variability of phytoplankton and relationship with production of CDOM in the polynya of the Amundsen Sea, Antarctica. Deep-Sea Res. II 123, 30–41.
Lee, S.H., Hwang, J., Ducklow, H.W., Hahm, D., Lee, S.H., Kim, D., Hyun, J.H., Park, J., Ha, H.K., Kim, T.W., 2017. Evidence of minimal carbon sequestration in the productive Amundsen Sea polynya. Geophys. Res. Lett. 44, 7892–7899.
Maie, N., Scully, N.M., Pisani, O., Jaffé, R., 2007. Composition of a protein-like fluorophore of dissolved organic matter in coastal wetland and estuarine ecosystems. Water Res. 41 (3), 563–570.
Mouginot, J., Rignot, E., Scheuchl, B., 2014. Sustained increase in ice discharge from the Amundsen Sea Embayment, West Antarctica, from 1973 to 2013. Geophys. Res. Lett. 41, 1576–1584.
Musilova, M., Tranter, M., Wadham, J., Telling, J., Tedstone, A., Anesio, A.M., 2017. Microbially driven export of labile organic carbon from the Greenland ice sheet. Nat. Geosci. 10, 360–365.
Ortega-Retuerta, E., Frazer, T.K., Duarte, C.M., Ruiz-Halpern, S., Tovar-Sánchez, A., Arrieta, J.M., Rechea, I., 2009. Biogeneration of chromophoric dissolved organic matter by bacteria and krill in the Southern Ocean. Limnol. Oceanogr. 54, 1941–1950.
Parsons, T.R., Maita, Y., Lalli, C.M., 1984. A Manual of Chemical and Biological Methods for Seawater Analysis. Pergamon Press, Oxford.
Redfield, A.C., 1958. The biological control of chemical factors in the environment. Am. Sci. 46, 230A–221.
Ritz, C., Edwards, T.L., Durand, G., Payne, A.J., Peyaud, V., Hindmarsh, R.C.A., 2015. Potential sea-level rise from Antarctic ice-sheet instability constrained by observations. Nature 528, 115–118.
Romera-Castillo, C., Letscher, R.T., Hansell, D.A., 2016. New nutrients exert fundamental control on dissolved organic carbon accumulation in the surface Atlantic Ocean. Proc. Natl. Acad. Sci. 113, 10497.
Rosario-Ortiz, F.L., Korak, J.A., 2017. Oversimplification of dissolved organic matter fluorescence analysis: potential pitfalls of current methods. Environ. Sci. Technol. 51 (2), 759–761.
Sabine, C.L., Feely, R.A., Gruber, N., Key, R.M., Lee, K., Bullister, J.L., Wanninkhof, R., Wong, C.S., Wallace, D.W.R., Tilbrook, B., 2004. The oceanic sink for anthropogenic CO_2. Science 305, 367.
Sallee, J.-B., Matear, R.J., Rintoul, S.R., Lenton, A., 2012. Localized subduction of anthropogenic carbon dioxide in the Southern Hemisphere oceans. Nat. Geosci. 5, 579–584.
Schaub, T.M., Rodgers, R.P., Marshall, A.G., 2005. Speciation of aromatic compounds in petroleum refinery streams by continuous flow field desorption ionization FT-ICR mass spectrometry. Energy Fuel 19, 1566–1573.
Schofield, O., Miles, T., Alderkamp, A.C., Lee, S., Haskins, C., Rogalsky, E., Sipler, R., Sherrell, R.M., Yager, P.L., 2015. In situ phytoplankton distributions in the Amundsen Sea Polynya measured by autonomous gliders. Elem. Sci. Anth. 3, 1–17.
Shen, Y., Benner, R., Murray, A.E., Gimpel, C., Mitchell, Greg B., Weiss, E.L., Reiss, C., 2017. Bioavailable dissolved organic matter and biological hot spots during austral winter in Antarctic waters. J. Geophys. Res. Oceans 122, 508–520.
Singer, G.A., Fasching, C., Wilhelm, L., Niggemann, J., Steier, P., Dittmar, T., Battin, T.J., 2012. Biogeochemically diverse organic matter in Alpine glaciers and its downstream fate. Nat. Geosci. 5 (10), 710–714.
Sinha, R.P., Singh, S.P., Häder, D.-P., 2007. Database on mycosporines and mycosporine-like amino acids (MAAs) in fungi, cyanobacteria, macroalgae, phytoplankton and animals. J. Photochem. Photobiol. B 89, 29–35.
Sipler, R.E., Connelly, T.L., 2015. Bioavailability of surface dissolved organic matter to aphotic bacterial communities in the Amundsen Sea Polynya, Antarctica. Elem. Sci. Anth. 3, 000060.
Smith, H.J., Foster, R.A., McKnight, D.M., Lisle, J.T., Littmann, S., Kuypers, M.M.M., Foreman, C.M., 2017. Microbial formation of labile organic carbon in Antarctic glacial environments. Nat. Geosci. 10, 356–359.
Song, H.J., Kang, J.J., Bo, K.K., Joo, H.T., Yang, E.J., Park, J., Sang, H.L., Sang, H.L., 2016. High protein production of phytoplankton in the Amundsen Sea. Deep-Sea Res. II 123, 50–57.
Spencer, R.G.M., Guo, W.D., Raymond, P.A., Dittmar, T., Hood, E., Fellman, J., Stubbins, A., 2014. Source and biolability of ancient dissolved organic matter in glacier and lake ecosystems on the Tibetan Plateau. Geochim. Cosmochim. Acta 142, 64–74.
Stedmon, C.A., Bro, R., 2008. Characterizing dissolved organic matter fluorescence with parallel factor analysis: a tutorial. Limnol. Oceanogr. Methods 6, 572–579.
Stedmon, C.A., Thomas, D.N., Papadimitriou, S., Granskog, M.A., Dieckmann, G.S., 2011. Using fluorescence to characterize dissolved organic matter in Antarctic sea ice brines. J. Geophys. Res. Biogeosci. 116, G03027.
St-Laurent, P., Klinck, J.M., Dinniman, M.S., 2013. On the role of coastal troughs in the circulation of warm circumpolar deep water on Antarctic shelves. J. Phys. Oceanogr. 43, 51–64.
Tamsitt, V., Drake, H.F., Morrison, A.K., Talley, L.D., Dufour, C.O., Gray, A.R., Griffies, S.M., Mazloff, M.R., Sarmiento, J.L., Wang, J., Weijer, W., 2017. Spiraling pathways of global deep waters to the surface of the Southern Ocean. Nat. Commun. 8, 172.
Tupas, L.M., Koike, I., Karl, D.M., Holm-Hansen, O., 1994. Nitrogen metabolism by heterotrophic bacterial assemblages in Antarctic coastal waters. Polar Biol. 14 (3), 195–204.
Turner, J., Orr, A., Gudmundsson, G.H., Jenkins, A., Bingham, R.G., Hillenbrand, C.D., Bracegirdle, T.J., 2017. Atmosphere-ocean-ice interactions in the Amundsen Sea embayment, West Antarctica. Rev. Geophys. 55, 235–276.
Wang, Y., Spencer, R.G.M., Podgorski, D.C., Kellerman, A.M., Rashid, H., Zito, P., Xiao, W., Wei, D., Yang, Y., Xu, Y., 2018. Spatiotemporal transformation of dissolved organic matter along an alpine stream flow path on the Qinghai–Tibet Plateau: importance of source and permafrost degradation. Biogeosciences 15 (21), 6637–6648.
Williams, C.M., Dupont, A.M., Loevenich, J., Post, A.F., Dinasquet, J., Yager, P.L., 2016. Pelagic microbial heterotrophy in response to a highly productive bloom of Phaeocystis antarctica in the Amundsen Sea Polynya, Antarctica. Elem. Sci. Anth. 4, 000102.
Yager, P.L., Sherrell, R.M., Stammerjohn, S.E., Ducklow, H.W., Schofield, O., Ingall, E.D., Wilson, S.E., Lowry, K.E., Williams, C.M., Riemann, L., 2016. A carbon budget for the Amundsen Sea Polynya, Antarctica: estimating net community production and export in a highly productive polar ecosystem. Elem. Sci. Anth. 4, 000140.
Yamashita, Y., Tanoue, E., 2003. Chemical characterization of protein-like fluorophores in DOM in relation to aromatic amino acids. Mar. Chem. 82 (3–4), 255–271.